

1 **Anchorless cell surface proteins function as laminin-binding adhesins in *Lactobacillus***
2 ***rhamnosus* FSMM22**

3
4 Ni Putu Desy Aryantini¹, Daisuke Kondoh², Keita Nishiyama^{3,5}, Yuji Yamamoto³, Takao Mukai³, I
5 Nengah Sujaya⁴, Tadasu Urashima¹, and Kenji Fukuda^{1,*}

6
7 ¹Department of Animal and Food Hygiene, Obihiro University of Agriculture and Veterinary Medicine,
8 Inada-cho, Obihiro, Hokkaido 080-8555, Japan.

9 ²Department of Basic Veterinary Medicine, Obihiro University of Agriculture and Veterinary
10 Medicine, Hokkaido 080-8555, Japan.

11 ³Department of Animal Science, School of Veterinary Medicine, Kitasato University, Towada, Aomori
12 034-8628, Japan.

13 ⁴Integrated Laboratory for Bioscience and Biotechnology, Udayana University, Bukit Jimbaran
14 Campus, Badung, Bali, Indonesia.

15 ⁵Current address: Department of Microbiology, School of Pharmacy, Kitasato University, Minato-ku,
16 Tokyo 108-8641, Japan.

17
18 *Corresponding author: Kenji Fukuda, Department of Animal and Food Hygiene, Obihiro University
19 of Agriculture and Veterinary Medicine, Inada-cho, Obihiro, Hokkaido 080-8555, Japan. Tel: +81-
20 155-49-5564; Fax: +81-155-49-5577; E-mail: fuku@obihiro.ac.jp

21
22 One sentence summary: Laminin-binding cell surface proteins in *Lactobacillus rhamnosus* FSMM22.

23
24 Keywords: cell surface proteins; host-microbial interactions; lactic acid bacteria; laminin; probiotics;
25 ribosomal proteins

26 **ABSTRACT**

27 Anchorless cell surface proteins (CSPs) were extracted with 1 M lithium chloride solution from
28 *Lactobacillus rhamnosus* FSMM22. Loss of the anchorless CSPs resulted in a two-fold decrease in
29 FSMM22 cells bound to a constitutive extracellular matrix glycoprotein, laminin, *in vitro*. DNA-
30 binding protein HU, glyceraldehyde-3-phosphate dehydrogenase, lactate dehydrogenase, and 30S
31 ribosomal protein S19 (RpsS) were identified by mass spectrometry in the extract as laminin-binding
32 adhesins. Among the four proteins, RpsS was immunohistochemically confirmed to exist on the cell
33 surface. Our findings strongly suggest that anchorless CSPs can enhance bacterial adhesion to the host.

34 **Introduction**

35 To achieve situational attachment/detachment to various adhesion sites on the host in response to
36 changes in the surrounding environment, commensal and pathogenic bacteria use several different
37 types of cell surface proteins (CSPs). For example, pilus adhesins (Lebeer et al. 2012) are cell wall
38 binding proteins that are strongly anchored to the bacterial cell wall (covalently bound through the
39 action of sortases, e.g. LPXTG proteins, or through non-covalent interactions). Another example is
40 anchorless proteins that associate weakly or moderately with the bacterial cell wall, such as
41 moonlighting proteins, which show multiple functions at different cellular localisation (Jeffery 1999;
42 Kainulainen and Korhonen 2014). However, the full composition of CSPs has not yet been determined
43 for any bacterial species, owing mainly to the wide variety and complexity of CSPs and their
44 counterparts.

45 *Lactobacillus rhamnosus* strains FSMM15 and FSMM22 were previously isolated from fermented
46 mare's milk as potential probiotics (Shi et al. 2012). These strains showed similar adhesion for porcine
47 colonic mucin compared to *Lactobacillus rhamnosus* GG ATCC 53103 (LGG). Moreover, compared
48 to FSMM15, FSMM22 showed about a 100-fold increase in the number of bacterial cells bound to the
49 laminin (Shi et al. 2012). Therefore, these two strains have the potential to serve as a model for
50 investigating the roles of CSPs in binding to laminin. A recent study by Nishiyama et al. (2015)
51 revealed that an anchored CSP, mucus-binding factor, was important for the binding of FSMM22 to
52 porcine colonic mucin and to some glycoproteins that compose the host's extracellular matrix protein
53 (ECM), including laminin. To identify a variety of CSPs in FSMM15 and FSMM22 and focus on their
54 binding properties to laminin, 1 M lithium chloride (LiCl) solution, which is commonly used for the
55 extraction of anchorless CSPs (Rojas et al. 2002), was used in this study.

56

57 **Materials and Methods**

58 **Bacterial cell culture**

59 LGG was purchased from the American Type Culture Collection (Manassas, VA, USA). Single
60 colonies of *L. rhamnosus* FSMM15 and FSMM22 from our culture collection and LGG were statically
61 pre-cultured in 15 mL of de Man-Rogosa-Sharpe (MRS) broth (Oxoid, Basingstoke, UK) for 20 h at
62 37°C. For the main culture, 0.4 to 1% of bacterial suspensions were inoculated into 250 mL of MRS
63 broth and incubated under anaerobic conditions using AnaeroPack Kenki (Mitsubishi Gas Chemical,
64 Tokyo, Japan). After incubation for 20 h at 37°C, cells were pelleted by centrifugation at $3,000 \times g$ for
65 15 min at 4°C, washed twice with phosphate buffered saline (PBS), and used in the following
66 experiments.

67

68 **CSP extraction and their effects on the laminin-adhesion properties of FSMM15 and FSMM22**

69 CSPs were extracted from bacterial cells by suspension in either 1 M LiCl solution or PBS for 1 h

70 at 4°C with agitation. Then, the suspension was centrifuged at $8,000 \times g$ for 30 min at 4°C, and the
71 supernatant was filtered through a nitrocellulose membrane (0.2- μm pore size, Advantec, Japan). The
72 filtrate was concentrated using Centriprep YM-3 (Merck Millipore, Billerica, MA, USA), dialyzed
73 against PBS with a 1-kDa molecular weight cut-off membrane (GE Healthcare, Chicago, IL, USA) at
74 4°C overnight, freeze dried, and kept at -30°C until use. Protein concentration was estimated
75 spectrophotometrically at 280 nm under the assumption of $E^{1\%}_{1\text{cm}} = 10$.

76 To evaluate the effects of CSP removal on the laminin-binding properties of the FSMM strains,
77 the bacterial cell number was determined before and after the extraction as previously described
78 (Nishiyama et al. 2015), with a modification that bacterial cells were harvested at the stationary phase.

79

80 **Inhibition enzyme-linked immunosorbent assay (ELISA)**

81 Inhibition ELISA was performed to detect laminin-binding proteins (LBPs) in the CSPs.
82 Approximately 2.5 μg of mouse laminin-111 (BD Biosciences, Bedford, MA, USA) was dissolved in
83 1 mL of 0.25 M carbonate-bicarbonate buffer (pH 9.6), and a 100- μL aliquot was added per well of a
84 96-well Maxisorp plate (Thermo Fisher Scientific, Waltham, MA, USA) and incubated overnight at
85 4°C. Unbound laminin was removed by washing with 0.1% Tween-20 in PBS (PBS-T). To prevent
86 unspecific binding of CSPs, wells were treated with 200 μL of 1% bovine serum albumin (BSA) in
87 PBS at 37°C for 2 h. Each of the lyophilized CSPs obtained from FSMM15 and FSMM22 was
88 reconstituted in 500 μL of 0.1% BSA in PBS; then the 100- μL aliquot was added and allowed to bind
89 to laminin at 37°C for 2 h. As a control, 100 μL of 0.1% BSA solution was used. Unbound CSPs were
90 removed by washing with PBS-T; next, 100 μL of chicken polyclonal anti-laminin antibody (Abcam,
91 Cambridge, UK; diluted 1:20,000 with 1% BSA in PBS) was added and incubated at 37°C for 2 h.
92 After removal of unbound anti-laminin antibody, 100 μL of goat anti-chicken IgY conjugated-
93 horseradish peroxidase (Abcam; diluted 1:10,000 with 1% BSA in PBS) was added and incubated for
94 1 h at room temperature (RT). The titre was measured at 492 nm using a Multiskan FC microplate
95 photometer (Thermo Fisher Scientific).

96

97 **Isolation and identification of LBPs**

98 LBPs were isolated from CSPs according to Muñoz-Provencio et al. (2011) with modifications.
99 Immobilization of laminin and the CSP binding reaction were performed as described above. In brief,
100 CSPs bound to the immobilized laminin were recovered with 60 μL of 1% (w/v) sodium dodecyl
101 sulfate (SDS) solution by incubation at RT for 2 h with agitation. The SDS solution was thoroughly
102 dried and the CSPs were recovered with 25 μL of Laemmli buffer (Laemmli 1970), denatured at 95°C
103 for 5 min, and then subjected to 12.5% SDS polyacrylamide gel electrophoresis (PAGE). A precision
104 plus protein dual color standard (Bio-Rad Laboratories, Hercules, CA, USA) was used as a protein
105 size marker. Protein bands were visualized using the Dodeca silver staining kit (Bio-Rad Laboratories)

106 according to the manufacturer's instruction and were then manually excised. Destaining of the gel
107 pieces, in-gel digestion of the proteins, and protein identification using a mass spectrometer were
108 performed as previously reported (Senda et al. 2011).

109

110 **Immunohistochemical staining**

111 A rabbit polyclonal antibody was prepared against a custom-made synthetic peptide for the N-
112 terminal 19 amino acid sequence, MGRSLKKGPFADAHLLKKI, of RpsS (GenBank ID:
113 BAI42919.1). A biotinylated anti-rabbit IgG raised in goats was purchased from Vector laboratories
114 (Burlingame, CA, USA). Dead cells were stained with 10 $\mu\text{g mL}^{-1}$ propidium iodide in PBS before
115 fixation. Harvested cells were washed with PBS and fixed in 4% paraformaldehyde in PBS at RT for
116 30 min. After incubation, cells were washed with PBS, and then incubated with 400 $\mu\text{g mL}^{-1}$ lysozyme
117 in PBS at 37°C for 30 min to partially degrade the cell wall. Then, cells were washed with PBS, and
118 one drop of the cell suspension was spotted onto a glass slide. After the solvent dried, cells were
119 washed with distilled water. To detect total cells, 4',6-diamidino-2-phenylindole (DAPI) staining was
120 performed, applying 10 $\mu\text{g mL}^{-1}$ DAPI in PBS at RT for 5 min. For immunohistochemical staining of
121 RpsS, cells were incubated with 0.3% H_2O_2 in methanol at RT for 30 min to eliminate endogenous
122 peroxidase activity and were also incubated with 3% normal goat serum at RT for 30 min to block
123 non-specific reactions. After removal of the goat serum, cells were incubated with anti-RpsS
124 antibodies (1:50 in dilution buffer) at RT for 2 h. After this incubation, cells were washed with PBS
125 and then incubated with the biotinylated anti-rabbit IgG (7.5 $\mu\text{g mL}^{-1}$ in dilution buffer) at RT for 1 h.
126 After washing with distilled water, cells were incubated with an avidin:biotinylated enzyme complex
127 (Vector laboratories) at RT for 30 min. For colour development, cells were incubated with PBS
128 containing 0.02% 3,3'-diaminobenzidine tetrahydrochloride (DAB) and 0.006% H_2O_2 .

129 The effects of artificial gastric and intestinal fluid treatment on the presence of cell-surface RpsS
130 were examined according to Fernandez et al. (2003). Approximately 10^{10} cells were incubated in 10
131 mL of artificial gastric juice (125 mM NaCl, 7 mM KCl, 45 mM NaHCO_3 , 3 g L^{-1} pepsin, pH 3.0).
132 The bacterial suspensions were incubated at 37°C anaerobically with agitation for 180 min. Then, the
133 cells were collected, suspended in 10 mL of artificial intestinal fluids (0.1% pancreatin, 0.15% oxgall
134 in distilled water, pH 8.0), incubated as previously described, and followed by immunohistochemical
135 staining.

136

137 **Quantification of *rpsS* mRNA levels in *Lactobacillus* strains using real-time RT-PCR**

138 Total RNA was extracted from FSMM15, FSMM22, and LGG at the mid-exponential growth
139 phase using RNeasy mini kit (Qiagen, Hilden, Germany) according to the manufacturer's instructions.
140 Reverse transcriptase polymerase chain reaction (RT-PCR) was performed to synthesize single strand
141 cDNA, according to the provided protocol. In this study, two housekeeping genes, *gapdh* and the 16S

142 rRNA gene, were used as internal controls to predict the relative expression level of *rpsS* genes.
143 Standard curves were constructed in duplicate using the PCR products of *rpsS*, *gapdh*, and 16S rRNA
144 gene using a single colony of LGG as a template. To obtain a 10-fold serial dilution in the range of
145 10^8 to 10^1 for real-time PCR, cDNA concentration was adjusted to 500 ng/ μ L of EB buffer (Qiagen),
146 diluted 10-fold, and subjected to real-time PCR reaction using Power CYBR Green PCR master mix
147 (Thermo Fisher Scientific). Real-time PCR was performed by using the STEP ONE plus real-time
148 PCR System (Thermo Fisher Scientific). The cycle conditions were as follows: 95°C for 10 min, 40
149 cycles of 95°C for 9 sec, 57.5°C or 60.5°C for 1 min, and followed by a dissociation step of 95°C for
150 15 sec, 60°C for 1 min, and 95°C for 15 sec to determine the arbitrarily-place threshold (C_T) values
151 of the amplicons. The gene copy numbers of the samples were analysed using the absolute
152 quantification method by extrapolating the C_T values of the samples and the standard curves. The
153 analysis was performed using StepOne software for StepOne and StepOnePlus real-time PCR system
154 Version 2.2.2. Primers used in this study are listed in Table 1.

155

156 **Western blotting**

157 Proteins in an SDS-PAGE gel were transferred to a polyvinylidene difluoride membrane using
158 mini-trans-blot electrophoretic transfer cell (Bio-Rad Laboratories). Blocking was performed with 5%
159 (w/v) blocking agent (GE Healthcare) in PBS-T at RT for 2 h. After rinsing with PBS-T, the membrane
160 was incubated with an anti-RpsS antibody (diluted 1:5,000) in PBS-T at 4°C overnight. After washing
161 with PBS-T, the membrane was incubated with horseradish peroxidase-conjugated goat anti-rabbit
162 IgG (diluted 1:50,000) at RT for 1 h. Signals were developed with ECL prime Western blotting
163 detection reagent (GE Healthcare) and analysed using Ez-Capture MG (Atto, Tokyo, Japan). An anti-
164 RNA polymerase antibody (diluted 1:1,000; Neoclone, Madison, WI, USA) was used to detect RNA
165 polymerase as a cytosolic protein marker.

166

167 **Statistical analysis**

168 Experiments were performed in triplicate from three independent cultures and expressed as the
169 mean \pm standard deviation. Cell viability and protein concentration were analysed by Student's t-test.
170 Analysis of variance with post-hoc Dunnet's test was used for ELISA experiments.

171

172 **Results**

173 **Profiles of CSPs extracted from FSMM15 and FSMM22 with 1 M LiCl**

174 CSPs yielded 143 ± 12 and 580 ± 60 μ g mL⁻¹ in FSMM15 and FSMM22, respectively. Cell
175 viabilities before and after extraction were 1.6×10^8 and 1.5×10^8 colony forming units (CFU) mL⁻¹
176 for FSMM15, respectively, and 1.3×10^8 and 1.2×10^8 CFU mL⁻¹ for FSMM22, respectively, indicating
177 that cell damage was negligible (Table S1). Removal of CSPs led to an approximately 2-fold decrease

Table 1

Table S1

178 in the laminin-binding ability of FSMM22 but not of FSMM15, indicating that CSPs act as laminin
179 adhesins on the cell surface (Fig. 1). As shown in Fig. 2, the band patterns of CSPs in FSMM15 and
180 FSMM22 1M LiCl extracts were highly similar. In contrast, proteins that bound to laminin were
181 present in trace amounts in FSMM15, whereas several bands were observed in FSMM22. The
182 FSMM22 CSPs extracted with 1M LiCl solution significantly decreased the ELISA titre compared to
183 that of the control (Fig. 3), supporting the result obtained through SDS-PAGE analysis. Mass
184 spectrometry analysis revealed that DNA-binding protein HU (HUP), glyceraldehyde-3-phosphate
185 dehydrogenase (GAPDH), lactate dehydrogenase (LDH), and 30S ribosomal protein S19 (RpsS) were
186 a part of the LBPs in the FSMM22 CSPs extracted with 1M LiCl solution (Fig. S1).

Fig. 1

Fig. 2

Fig. 3

Fig. S1

187

188 **Detection of RpsS present on the cell surface of FSMM22 by immunohistochemical staining**

189 The binding specificity of the primary antibody was confirmed by Western blotting (Fig. S2). RpsS
190 was clearly detected in the cell surface region of FSMM22 but not in FSMM15 (Fig. 4). The number
191 of RpsS on the surface of living FSMM22 cells decreased after the cells were damaged by treatment
192 with artificial gastric and intestinal fluids, because the thickness of the DAB-stained dark brown layer
193 surrounding the bacterial cells apparently decreased. Binding of the primary antibody against RpsS
194 was inhibited under the presence of the antigen peptide (Fig. S3).

Fig. S2

Fig. 4

Fig. S3

195

196 **Gene and protein expression levels of RpsS in *L. rhamnosus* FSMM15 and FSMM22**

197 To better understand the different RpsS numbers on the cell surface of FSMM15 and FSMM22
198 cells, the mRNA and protein expression levels of RpsS in the two strains were investigated.
199 Consequently, there was no significant difference in the expression level of *rpsS* during the mid-
200 exponential growth phase of FSMM15 and FSMM22; *gapdh* and 16S rRNA genes were used as
201 controls (Fig. 5A). In contrast, RpsS was detectable in the 1 M LiCl and cell-free FSMM22 extracts
202 but not in FSMM15 extracts (Fig. 5B).

Fig. 5

203

204 **Discussion**

205 Nishiyama et al. (2015) reported that a FSMM22 mucus-binding protein deletion mutant lost one-
206 half of its laminin-binding ability; therefore, our results suggest that the other half should be attributed
207 to anchorless CSPs that are extractable with 1 M LiCl. FSMM15 adhered to laminin to some extent
208 (Shi et al. 2012), despite the lower amount of extracted LBPs in FSMM15 compared to that in
209 FSMM22; thus, FSMM15 may express different types of CSPs, such as *lmb*, a LBP found in
210 *Streptococcus agalactiae* (Spellerberg et al. 1999) and laminin-binding microbial surface components
211 recognizing adhesive matrix molecules (Sillanpää et al. 2004). The distribution of CSPs responsible
212 for adhesion to the host seems to be bacterial strain dependent as was previously reported (Mackenzie
213 et al. 2010). Whether the FSMM strains are piliated is unknown. Laminin-binding ability has already

214 been described for GAPDH, which associates with the cell wall of *Candida albicans* (Gozalbo et al.
215 1998). It is also likely for HUP because an HUP homolog in *Mycobacterium tuberculosis* showed 78%
216 identity of amino acids towards a 21-kDa LBP found in *Mycobacterium leprae* (Shimoji et al. 1999).
217 LDH is also known to function as a moonlighting protein, e.g. an eye lens protein in geckos (van
218 Rheede et al. 2003); however, there is currently no report in relation to laminin binding. Further
219 experiments are needed to confirm the laminin-binding ability of LDH given the possibility of
220 complex formation between LDH and GAPDH, as was found in a multicomponent Oct-1 coactivator
221 that is essential for S phase-dependent histone H2B transcription (Zheng et al. 2003), cannot be
222 excluded. Previously reported laminin binding moonlighting proteins, such as enolase (Antikainen et
223 al. 2007a), glutamine synthetase (Kainulainen et al. 2012), and malate synthase (Kinhikar et al. 2006),
224 were not found in this study.

225 RpsS is a small protein with an approximate molecular mass of 10,000 that exists in a complex
226 with 30S ribosomal protein S13, which binds to 16S rRNA in the prokaryotic small ribosomal subunit
227 (Schwarzbauer and Craven 1985). Among lactic acid bacteria, RpsS has been found on the cell surface
228 of *Lactococcus lactis* NZ900 grown in M17 medium supplemented with 0.5% glucose (Berlec et al.
229 2011) and *L. rhamnosus* grown under heavy metal stress (Sreevani et al. 2014), while 30S ribosomal
230 protein S5 was abundantly present in the surface-exposed proteome of LGG after bile stress
231 (Koskeniemi et al. 2011). Extraribosomal functions of ribosomal proteins have been well studied;
232 these functions expand beyond protein synthesis to encompass many biological processes, including
233 replication, transcription, and RNA processing (Wool 1996). Thus far, laminin-binding ability has been
234 attributed to the 40S ribosomal protein SA, which is a 67-kDa laminin receptor in vertebrates (Auth
235 and Brawerman 1992; Ardini et al. 1998). Although our data strongly suggest that the RpsS moonlights
236 on the cell surface as an LBP, further experiments are needed, e.g. inhibition of bacterial cell adhesion
237 to laminin using an appropriate anti-RpsS antibody. However, our preliminary experiment attempting
238 to inhibit FSMM22 adherence to immobilized laminin through the addition of anti-RpsS antibodies
239 was unsuccessful (Fig S4). Immunohistochemical staining was successful only when the bacterial cell
240 wall peptidoglycan was partially degraded by lysozyme; therefore, the binding epitope seems to not
241 be exposed to the solvent, and this might be the reason why the preliminary experiment did not succeed.

242 There was no significant difference between the mRNA expression levels of the *rpsS* gene in
243 FSMM15 and FSMM22. On the other hand, no positive band could be detected even in the cell-free
244 extract of FSMM15 by Western blotting analysis, implying the occurrence of an unknown variation in
245 the N-terminal region of FSMM15 RpsS. These observations led us to assume the existence of a
246 specific RpsS transport pathway from the cytosol to the cell surface of FSMM22 cells, although further
247 experiments are needed. In fact, the molecular mechanism of transporting anchorless CSPs is
248 controversial. There is experimental evidence to support the presence of an unknown export pathway
249 of moonlighting proteins (Boël et al. 2005), secretion from dead or traumatized cells (Stephenson et

Fig. S4

250 al. 1999), and increased membrane permeability (Saad et al. 2009). These alternatives are not entirely
251 mutually exclusive as mentioned by Kainulainen and Korhonen (2014). RpsS is a highly basic protein
252 with a theoretical *pI* value of around 10, which may support its presence on the bacterial cell surface
253 *via* electrostatic interaction; however, the pH-dependent attachment/detachment observed in acidic
254 enolase (*pI* = 4.8) and GAPDH (*pI* = 5.2) from *Lactobacillus crispatus* (Antikainen et al. 2007b) is
255 not likely the case for RpsS.

256 To summarize, HUP, GAPDH, LDH, and RpsS were extractable with 1 M LiCl in *L. rhamnosus*
257 FSMM22, but not FSMM15, as a part of CSPs that enhanced the bacterial adhesion to laminin. The
258 cell surface localisation of RpsS in lactobacilli was immunohistochemically confirmed for the first
259 time. Our findings suggest that the host-bacterial interaction is influenced by the abundance of
260 anchorless CSPs in addition to contributions by pilus adhesins and anchored CSPs.

261 **REFERENCES**

- 262 Antikainen J, Kuparinen V, Lähteenmäki K, et al. Enolases from Gram-positive bacterial pathogens
263 and commensal lactobacilli share functional similarity in virulence-associated traits. *FEMS*
264 *Immunol Med Microbiol* 2007a;**51**:526-34.
- 265 Antikainen J, Kuparinen V, Lähteenmäki K, et al. pH-dependent association of enolase and
266 glyceraldehyde-3-phosphate dehydrogenase of *Lactobacillus crispatus* with the cell wall and
267 lipoteichoic acids. *J Bacteriol* 2007b;**189**:4539-43.
- 268 Ardini E, Pesole G, Tagliabue E, et al. The 67-kDa laminin receptor originated from a ribosomal
269 protein that acquired a dual function during evolution. *Mol Biol Evol* 1998;**15**:1017-25.
- 270 Auth D, Brawerman G. A 33-kDa polypeptide with homology to the laminin receptor: component of
271 translation machinery. *Proc Natl Acad Sci U S A* 1992;**89**:4368-72.
- 272 Berlec A, Zadavec P, Jevnikar Z, et al. Identification of candidate carrier proteins for surface display
273 on *Lactococcus lactis* by theoretical and experimental analyses of the surface proteome. *Appl*
274 *Environ Microbiol* 2011;**77**:1292-300.
- 275 Boël G, Jin H, Pancholi V. Inhibition of cell surface export of group A streptococcal anchorless surface
276 dehydrogenase affects bacterial adherence and antiphagocytic properties. *Infect Immun*
277 2005;**73**:6237-48.
- 278 Fernández MF, Boris S, Barbés C. Probiotic properties of human lactobacilli strains to be used in the
279 gastrointestinal tract. *J Appl Microbiol* 2003;**94**:449-55.
- 280 Frank JA, Reich CI, Sharma S, et al. Critical evaluation of two primers commonly used for
281 amplification of bacterial 16S rRNA genes. *Appl Environ Microbiol* 2008;**74**:2461-70.
- 282 Gozalbo D, Gil-Navarro I, Azorín I, et al. The cell wall-associated glyceraldehyde-3-phosphate
283 dehydrogenase of *Candida albicans* is also a fibronectin and laminin binding protein. *Infect Immun*
284 1998;**66**:2052-9.
- 285 Jeffery CJ. Moonlighting proteins. *Trends Biochem Sci* 1999;**24**:8-11.
- 286 Kainulainen V, Loimaranta V, Pekkala A, et al. Glutamine synthetase and glucose-6-phosphate
287 isomerase are adhesive moonlighting proteins of *Lactobacillus crispatus* released by epithelial
288 cathelicidin LL-37. *J Bacteriol* 2012;**194**:2509-19.
- 289 Kainulainen V, Korhonen TK. Dancing to another tune-adhesive moonlighting proteins in bacteria.
290 *Biology (Basel)* 2014;**3**:178-204.
- 291 Kinhikar AG, Vargas D, Li H, et al. Mycobacterium tuberculosis malate synthase is a laminin-binding
292 adhesin. *Mol Microbiol* 2006;**60**:999-1013.
- 293 Koskenniemi K, Laakso K, Koponen J, et al. Proteomics and transcriptomics characterization of bile
294 stress response in probiotic *Lactobacillus rhamnosus* GG. *Mol Cell Proteomics*
295 2011;**10**:M110.002741.
- 296 Laemmli UK. Cleavage of structural proteins during the assembly of the head of bacteriophage T4.

297 *Nature* 1970;**227**:680-5.

298 Lebeer S, Claes I, Tytgat HL, et al. Functional analysis of *Lactobacillus rhamnosus* GG pili in relation
 299 to adhesion and immunomodulatory interactions with intestinal epithelial cells. *Appl Environ*
 300 *Microbiol* 2012;**78**:185-93.

301 Mackenzie DA, Jeffers F, Parker ML, et al. Strain-specific diversity of mucus-binding proteins in the
 302 adhesion and aggregation properties of *Lactobacillus reuteri*. *Microbiology* 2010;**156**:3368-78.

303 Muñoz-Provencio D, Pérez-Martínez G, Monedero V. Identification of surface proteins from
 304 *Lactobacillus casei* BL23 able to bind fibronectin and collagen. *Probiotics Antimicrob Proteins*
 305 2011;**3**:15-20.

306 Nishiyama K, Nakamata K, Ueno S, et al. Adhesion properties of *Lactobacillus rhamnosus* mucus-
 307 binding factor to mucin and extracellular matrix proteins. *Biosci Biotechnol Biochem* 2015;**79**:271-
 308 9.

309 Perkins DN, Pappin DJ, Creasy DM, et al. Probability-based protein identification by searching
 310 sequence databases using mass spectrometry data. *Electrophoresis* 1999;**20**:3551-67.

311 Rojas M, Ascencio F, Conway PL. Purification and characterization of a surface protein from
 312 *Lactobacillus fermentum* 104R that binds to porcine small intestinal mucus and gastric mucin. *Appl*
 313 *Environ Microbiol* 2002;**68**:2330-6.

314 Saad N, Urdaci M, Vignoles C, et al. *Lactobacillus plantarum* 299v surface-bound GAPDH: a new
 315 insight into enzyme cell walls location. *J Microbiol Biotechnol* 2009;**19**:1635-43.

316 Schwarzbauer J, Craven GR. Evidence that *E. coli* ribosomal protein S13 has two separable functional
 317 domains involved in 16S RNA recognition and protein S19 binding. *Nucleic Acids Res*
 318 1985;**13**:6767-86.

319 Senda A, Fukuda K, Ishii T, et al. Changes in the bovine whey proteome during the early lactation
 320 period. *Anim Sci J* 2011;**82**:698-706.

321 Shi T, Nishiyama K, Nakamata K, et al. Isolation of potential probiotic *Lactobacillus rhamnosus*
 322 strains from traditional fermented mare milk produced in Sumbawa Island of Indonesia. *Biosci*
 323 *Biotechnol Biochem* 2012;**76**:1897-903.

324 Shimoji Y, Ng V, Matsumura K, et al. A 21-kDa surface protein of *Mycobacterium leprae* binds
 325 peripheral nerve laminin-2 and mediates Schwann cell invasion. *Proc Natl Acad Sci U S A* 1999
 326 **96**:9857-62.

327 Sillanpää J, Xu Y, Nallapareddy SR, et al. A family of putative MSCRAMMs from *Enterococcus*
 328 *faecalis*. *Microbiology* 2004;**150**:2069-78.

329 Spellerberg B, Rozdzinski E, Martin S, et al. Lmb, a protein with similarities to the LraI adhesin family,
 330 mediates attachment of *Streptococcus agalactiae* to human laminin. *Infect Immun* 1999;**67**:871-8.

331 Sreevani S, Chandrasekhar K, Pramoda Kumari J. Structural dynamics of *Lactobacillus rhamnosus*
 332 proteins under copper sulphate and zinc chloride stress. *IJPSR* 2014;**5**:4233-9.

- 333 Stephenson K, Bron S, Harwood CR. Cellular lysis in *Bacillus subtilis*; the effect of multiple
334 extracellular protease deficiencies. *Lett Appl Microbiol* 1999;**29**:141-5.
- 335 van Rheede T, Amons R, Stewart N, et al. Lactate dehydrogenase A as a highly abundant eye lens
336 protein in platypus (*Ornithorhynchus anatinus*): epsilon (v)-crystallin. *Mol Biol Evol* 2003;**20**:994-
337 8.
- 338 Wool IG. Extraribosomal functions of ribosomal proteins. *Trends Biochem Sci* 1996;**21**:164-5.
- 339 Zheng L, Roeder RG, Luo Y. S phase activation of the histone H2B promoter by OCA-S, a coactivator
340 complex that contains GAPDH as a key component. *Cell* 2003;**114**:255-66.

341 **Figure legends**

342 **Fig. 1. Effects of CSP removal on the adhesive properties of *L. rhamnosus* FSMM15 and**
343 **FSMM22 on laminin.** Filled bars, relative bacterial cell numbers that bound to laminin prior to 1 M
344 LiCl extraction; diagonal bars, relative bacterial cell numbers that bound to laminin after 1M LiCl
345 extraction. The asterisk represents a statistically significant difference with $p < 0.05$ ($n = 3$).
346

347 **Fig. 2. SDS-PAGE profiles of the CSPs and LBPs extracted with 1 M LiCl from *L. rhamnosus***
348 **FSMM15 and FSMM22.** CSPs, cell surface proteins; LBPs, laminin-binding proteins; control, 0.1%
349 BSA in PBS was used in the isolation procedure of LBPs instead of CSP solution; size marker, a
350 precision plus protein dual color standard from 10-250 kDa (Bio-Rad Laboratories). Protein bands
351 were visualized by silver staining. The bands indicated by numbers were subjected to protein
352 identification by mass spectrometry analysis. GAPDH and LDH were found in band 5, whereas RpsS
353 and HUP were detected in band 8.
354

355 **Fig. 3. Inhibition ELISA using the CSPs extracted with 1 M LiCl from *L. rhamnosus* FSMM15**
356 **and FSMM22.** As a control, 0.1% BSA in PBS (filled bar) was used for ELISA, whereas the CSP
357 solutions were extracted with either PBS (diagonal bars) or 1 M LiCl (dotted bars) as described in the
358 Materials and Methods. When proteins in the CSP solutions bound to the immobilized laminin, binding
359 of the primary antibody to the immobilized laminin was hampered, and thereby, the titre showed a
360 significant decrease compared to that in the control. The asterisk represents a statistically significant
361 difference to the control with $p < 0.001$ ($n = 3$).
362

363 **Fig. 4. Anti-RpsS immunohistochemical staining of *L. rhamnosus* FSMM15 and FSMM22.**
364 'Before' and 'After' indicate before and after treatment with artificial gastric and intestinal fluids,
365 respectively. DAPI, PI, and Anti-RpsS indicate microscopic images of the bacterial cells stained with
366 4',6-diamidino-2-phenylindole, propidium iodide, and 3,3'-diaminobenzidine tetrahydrochloride,
367 respectively. Identical microscopic fields are shown for each staining method. Areas in which viable
368 cells were observed (stained not with PI but with DAPI) were squared in the DAB staining images and
369 are shown at higher magnification (High mag). White bars in the DAPI staining images represent a
370 length of 1 μm .
371

372 **Fig. 5. Expression levels of RpsS (A) mRNA and (B) protein in *L. rhamnosus* FSMM15 and**
373 **FSMM22.** In panel (A), the *rpsS* mRNA expression levels of the two FSMM strains were evaluated
374 by real-time RT-PCR using the 16S rRNA (filled bars) and *gapdh* (diagonal bars) genes as controls.
375 Error bars in the graphs represent the standard deviation ($n = 3$). In panel (B), the presence of RpsS in
376 the 1 M LiCl extracts and in the cell-free extracts is shown. The cell-free extracts were prepared from

377 bacterial cells obtained from 100 mL of the 20-h-culture broth. Cells were harvested, suspended in 20
378 mL of PBS, and then sonicated (20% amplitude for 3 min with 1 min interval, 7 times, on ice) using
379 the Vibra-Cell VC505 (Sonics & Materials, Newtown, CT, USA).

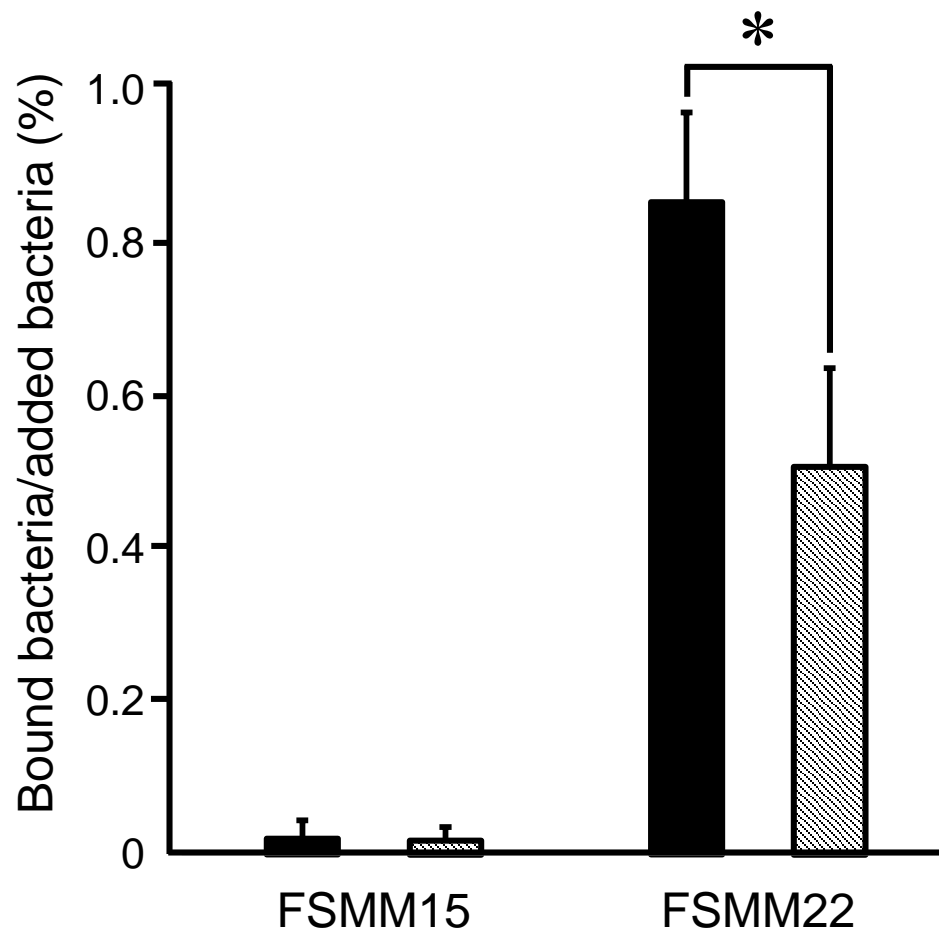


Fig. 1. Aryantini et al.

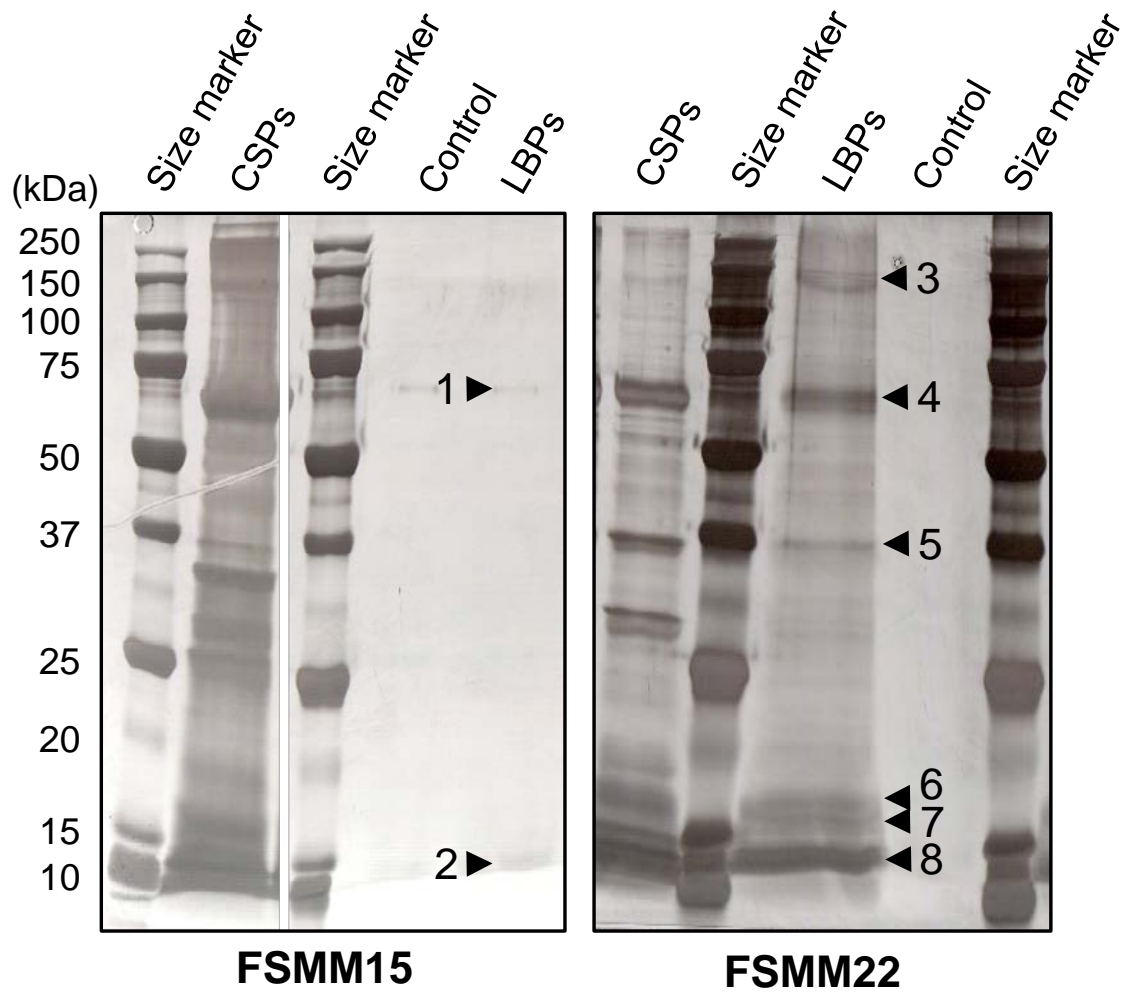


Fig. 2. Aryantini et al.

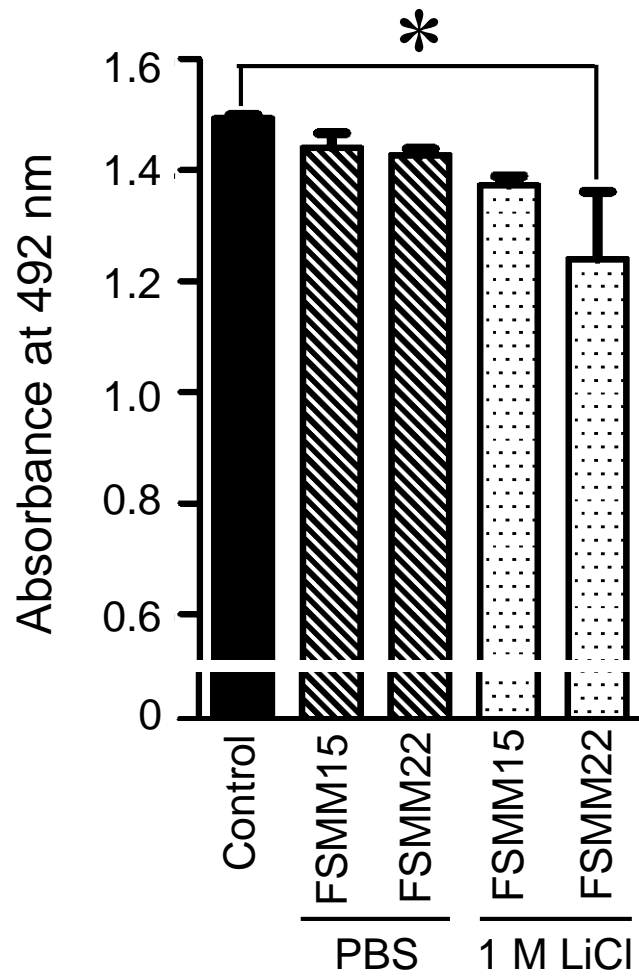


Fig. 3. Aryantini et al.

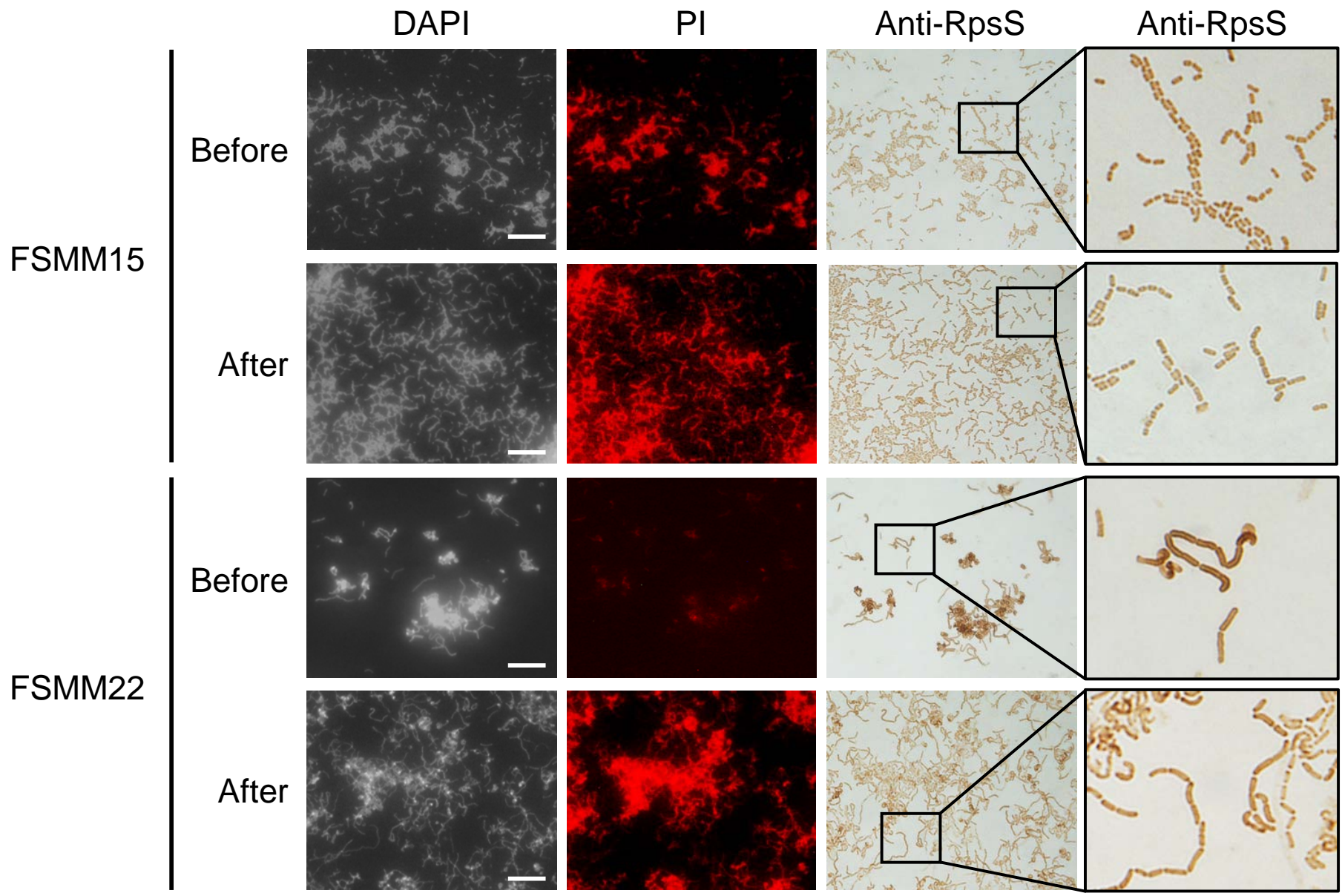
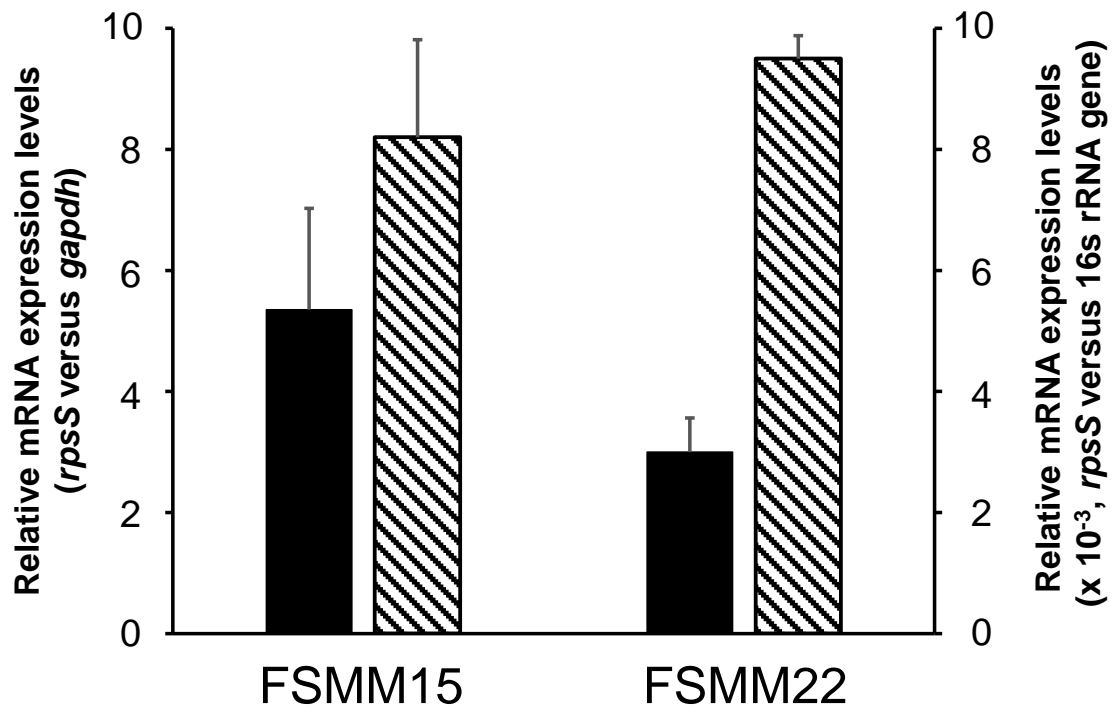


Fig. 4. Aryantini et al.

(A)



(B)

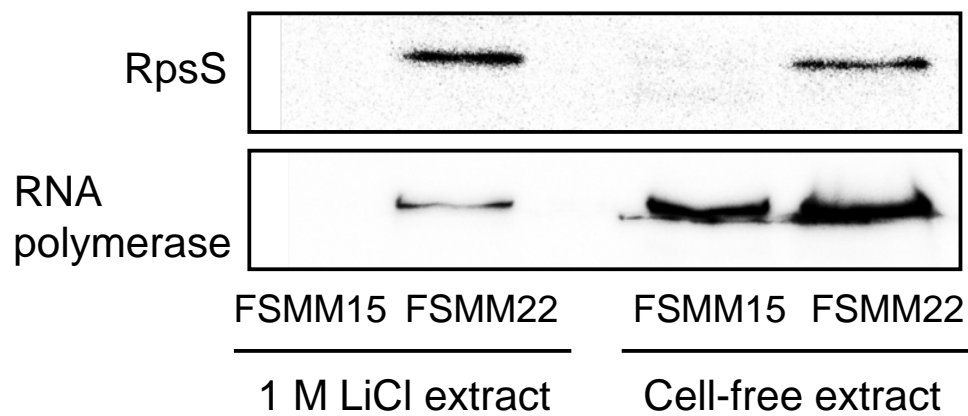


Fig. 5. Aryantini et al.

Table 1. Primers used in this study for real-time RT-PCR.

Genes ¹⁾	Primers	Sequence (5'→3')	Length (bp)	T _m (°C)	GC (%)	Amplicon size (bp)
<i>rpsS</i> (gi 258506995)	rpsS-F	ATGGGTCGCAGTCTTAAAAAAG	22	54	40.9	282
	rpsS-R	CTAGCGTGCTGTGTCTTCTTGTC	24	60	50.0	
	rpsS qPCR-F	TACACCATCGCCGTTTAC	18	54	50.0	82
	rpsS qPCR-R	TTCGCCTAACTTGTGACC	18	54	50.0	
<i>16s rRNA</i> (gi 507147971)	27F ²⁾	AGAGTTTGATCCTGGCTCAG	20	56	50.0	1528
	1492R ²⁾	TACCTTGTTACGACTT	16	45	37.5	
	16s rRNA qPCR-F	GTAGGGAATCTTCCACAATGGACG	24	60	50.0	321
16s rRNA qPCR-R	GTTCCACTGTCCTCTTCTGCAC	22	61	54.5		
<i>gapdh</i> (gi 258506995)	gapdh-F	TACTTCCCTGGTGAAGTTAGT	22	54	40.9	533
	gapdh-R	CCTGTAACTTGCCGTTCAATTC	22	57	45.5	
	gapdh qPCR-F	CAAAGCGTGTCTGATTTCTGC	22	57	45.5	158
	gapdh qPCR-R	CCTGGTTCAGGAAGTAAGCC	20	58	55.0	

¹⁾GenBank accession numbers are in parentheses.

²⁾Frank et al.